SCCS-527

On generalized cluster algorithms for frustrated spin models

P.D. Coddington

Northeast Parallel Architectures Center, 111 College Place,

Syracuse University, Syracuse, NY 13244, U.S.A.

L. Han

Physics Department, Syracuse University, Syracuse, NY 13244, U.S.A.

November 5, 1993

Standard Monte Carlo cluster algorithms have proven to be very effective for many different spin models, however they fail for frustrated spin systems. Recently a generalized cluster algorithm was introduced that works extremely well for the fully frustrated Ising model on a square lattice, by placing bonds between sites based on information from plaquettes rather than links of the lattice. Here we study some properties of this algorithm and some variants of it. We introduce a practical methodology for constructing a generalized cluster algorithm for a given spin model, and investigate apply this method to some other frustrated Ising models. We find that such algorithms work well for simple fully frustrated Ising models in two dimensions, but appear to work poorly or not at all for more complex models such as spin glasses.

I. INTRODUCTION

The cluster update algorithms of Swendsen and Wang [1] and Wolff [2] can provide a great improvement in computational efficiency over the Metropolis algorithm [3, 4] and other local Monte Carlo update schemes. Due to the non-local nature of the cluster algorithms, which update large clusters of spins at a time, they are very effective at decorrelating successive configurations and can therefore greatly reduce critical slowing down [4, 5] in certain ferromagnetic and anti-ferromagnetic spin models. However the cluster algorithms are ineffective for frustrated spin models [6] such as spin glasses [7], the systems for which critical slowing down can be most extreme, and for which a non-local update algorithm would be of most benefit. The reason for this failure is that at the critical point, these algorithms produce a cluster that encompasses a large fraction (if not all) of the sites in the lattice, so that updating the spins in this cluster is virtually the same as a trivial global spin update.

Kandel, Ben-Av and Domany (KBD) introduced a generalized cluster algorithm [8, 9] that includes the other cluster algorithms as special cases. Their method also works very well for the two dimensional fully frustrated Ising model [8, 10], but has not been applied to any other frustrated spin models. The only other cluster algorithm that has been shown to work effectively for a frustrated spin model is the Replica Monte Carlo algorithm [11], however this has only been successfully applied to the 2-d Ising spin glass [12]. It is therefore of great interest to determine whether the generalized cluster algorithm can be applied to other frustrated spin models. We have investigated some variants of the KBD algorithm for the 2-d fully frustrated Ising model (FFIM), and attempted to apply the method to some other frustrated two dimensional Ising models.

We introduce a practical method for constructing a generalized cluster algorithm for a given spin model in section II. We then apply this methodology to the FFIM on a square lattice in section III, the triangular lattice Ising anti-ferromagnet in section IV, and the 2-d Ising spin glass in section V. We analyze the performance of the generalized cluster algorithms for each of these models.

II. THE GENERALIZED CLUSTER ALGORITHM

First we briefly describe the Swendsen-Wang (SW) cluster algorithm for the Ising model [4], which has an interaction energy given by

$$E = -\sum_{<i,j>} J_{ij}\sigma_i\sigma_j, \tag{1}$$

where the spins σ_i can take the values $+1$ or -1. We will consider the case where the interaction strength J_{ij} takes on values $+J$ or $-J$, for some constant parameter $J > 0$. Let us define a link to be the connection between two neighboring sites on the lattice. A link is said to be satisfied if it is in a state of minimum energy, which means that the spins on the two sites are the same for $J_{ij} > 0$ or opposite for $J_{ij} < 0$, otherwise it is unsatisfied. In the SW algorithm, bonds are introduced between spins on neighboring sites with probability $1-e^{-2K}$ if the link is satisfied, and 0 if it is unsatisfied. Here $K = J/kT$ is a dimensionless coupling constant, where T is the temperature and k is Boltzmann's constant. This procedure creates clusters of bonded sites. The update part of the algorithm consists of flipping all the spins in a cluster (i.e. $\sigma_i \to -\sigma_i$) with probability $\frac{1}{2}$. Since the clusters can be quite large, this clearly produces large, non-local changes in the spin configuration, and thus decorrelates the configurations much faster than local update algorithms.

This algorithm works very well for the ferromagnetic ($J_{ij} = +J$) and anti-ferromagnetic ($J_{ij} = -J$) Ising model, but fails for frustrated systems, which have a mixture of positive and negative couplings in such a way that it is not possible for all links to be satisfied in the ground state. The simple reason for this failure is that the critical point for such systems usually occurs at low temperature (i.e. large K), where the probability of putting a bond on a satisfied link is close to 1. For example, the two dimensional fully frustrated Ising model has a critical point at zero temperature, where there are 3 satisfied links per plaquette. Hence the SW algorithm bonds each site to 3 of its neighbors on average, which results in all the sites in the lattice being connected into a single cluster. A more fundamental reason for this problem is that the SW algorithm only uses information from links, from which it is not possible to see the frustration in the system. To do that one needs information from the spins over at least a plaquette, which is the basic idea behind the KBD algorithm.

The generalized cluster algorithm begins by expressing the energy of the system as a sum $E = \sum_l V_l$. We will consider l to label subregions of the lattice such as links, plaquettes, or some other group of sites that can give a tiling of the lattice, that is, they can be replicated over the lattice in such a way that each link is part of one (and only one) subregion. We will refer to such a subregion as a *tile*. For each tile l we stochastically assign one of n possible operations with a probability $P_i^l(u)$ that depends on the spin configuration u and the operation i. These operations involve placing bonds between certain sites in the tile l. We refer to the placement (or non-placement) of bonds as *freezing* (or *deleting*) the connections between two neighboring sites. The frozen bonds produce clusters of connected sites. The probabilities must of course satisfy

$$\sum_i P_i^l(u) = 1, \qquad 0 \leq P_i^l(u) \leq 1, \tag{2}$$

for all l and u. KBD show that detailed balance is satisfied if the probabilities also satisfy [9]

$$E(u) - \frac{1}{\beta} \log P_i(u) + C_i = \begin{cases} 0 & \text{for an allowed operation } i \\ \infty & \text{otherwise.} \end{cases} \tag{3}$$

Here $E(u)$ is the energy for the configuration u, C_i is a constant (independent of the configuration), $\beta = 1/kT$ is the inverse temperature, and we have suppressed the subscript l labeling the particular tile. To simplify matters we will concentrate on a special case of the KBD generalized cluster algorithm, and define an operation as *allowed* if it does not freeze any unsatisfied links of the configuration u (for a more general definition, see Ref. [9]). If we define $a_i(u)$ to be 1 if operation i is allowed for configuration u, and 0 otherwise, then equation 3 can be written as

$$P_i(u) = a_i(u)\, e^{\beta(E(u)+C_i)}. \tag{4}$$

Imposing the normalization condition of equation 2, we have

$$\sum_i a_i(u)\, c_i = e^{-\beta E(u)} \qquad \forall\, u\,, \qquad\qquad c_i = e^{\beta C_i}. \tag{5}$$

This can be conveniently written as a matrix equation

$$\mathbf{A}\,\mathbf{c} = \mathbf{b}, \tag{6}$$

where the c_i are the elements of the vector $\mathbf{c}$, the Boltzmann factors $b_j = e^{-\beta E(u)}$ are the elements of the vector $\mathbf{b}$, and the $a_i(u)$ make up the elements A_{ij} of the *allowance matrix* $\mathbf{A}$, with j labeling the different possible configurations u.

Formulating a generalized cluster algorithm involves identifying some candidate operations, constructing the allowance matrix $\mathbf{A}$, and then solving the matrix equation 6 for $\mathbf{c}$, from which the probabilities for each operation can be calculated via equation 4. For a given set of operations and configurations, there is no guarantee that a solution to the matrix equation will exist. Even if the equation has a solution, it is quite likely that it will not satisfy the constraint that all the probabilities must be between 0 and 1. For all but the simplest models and tiles, the number of possible operations will be large, and the difficulty in this method is in choosing some subset of operations that allow a valid solution to the matrix equation. Here we offer some guidelines for choosing operators in order to maximize the possibility of obtaining a valid algorithm. Examples of this procedure will be given in the following sections.

Clearly the simplest way to approach the problem is to choose the operations so that the allowance matrix is square (the same number of operations as configurations) and upper triangular. This will guarantee a solution, although it may not satisfy the constraint that the probabilities are all between 0 and 1. A quick preliminary check to see if this constraint is violated is to check whether any of the elements of the solution vector **c** are negative, which is not allowed since $c_i = e^{C_i}$.

There will generally be more than one operation available for a given configuration which will produce an upper triangular allowance matrix. For frustrated models, we want to choose the operation which freezes the least number of bonds, and bonds together the fewest sites into the same cluster. However in some cases it is advantageous to choose more than one such operation for a given configuration. This gives a system of equations that is under-determined, that is, there are more unknowns than equations, producing free parameters in the solution. Having free parameters to play with is extremely useful: firstly, we may change an invalid solution into one that obeys the probability constraints; secondly, it may allow some optimization in the algorithm by tuning the size of the largest cluster, as done by KBD for the FFIM [8, 10]. Also, if an operation i only occurs for a single configuration, there are no constraints on the choice of C_i, which also gives a free parameter in choosing the probabilities.

For frustrated spin models, we are usually interested in simulating the system at low temperature. A good method of constructing an algorithm in this case is to start with a simpler zero temperature algorithm. In this case we only need consider the ground state configurations, and those operations that conserve the energy of these configurations. This greatly simplifies the problem of determining valid solutions, and also allows a quicker indication of whether the algorithm can produce a good distribution of cluster sizes. If the implemented zero temperature algorithm produces clusters that are neither too large nor too small, then an extended algorithm should work even better at non-zero temperature where the largest cluster will be smaller.

It should be possible to automate the procedure for constructing a valid generalized cluster algorithm. Given a particular spin model, a particular lattice, and a particular tiling of the lattice, a program could generate all possible configurations of the tile, and all possible allowed operations on those configurations. The program could then pick one possible choice of operations that give an upper triangular allowance matrix, possibly including some redundant operations to allow free parameters in the solution. It could then solve the matrix equation, calculate the probabilities, and check that the constraints on them are satisfied (this could all be done using a symbolic algebra package such as Mathematica [13]). If not, it could choose a new set of operations and repeat the procedure, until it finds a valid solution, or exhausts the list of operations. So far we have done most of this process by hand, however the steps involved appear amenable to automation.

III. THE SQUARE LATTICE FULLY FRUSTRATED ISING MODEL

The fully frustrated Ising model (FFIM) was introduced by Villain [14], as a simple regular frustrated system lacking the extra complication of disorder that is present in systems such as spin glasses. On a square lattice, the FFIM has ferromagnetic couplings on all links except for a line of anti-ferromagnetic couplings on every second column of links. This means that every plaquette is frustrated, having 3 ferromagnetic links and one anti-ferromagnetic link.

The critical point of this model is at zero temperature, where the configurations have one unsatisfied link per plaquette. The SW algorithm for this model puts a bond on all satisfied links, so there is only one unbonded link per plaquette. It is easy to prove (using the method of Kandel and Domany [10]) that in this case all the sites are bonded into a single cluster. Consider the dual lattice, where there is a site centered in each plaquette, and dual links which connect these dual sites, so that each dual link crosses (at right angles) a single link of the original lattice. Let us put bonds on the dual links which cross through unbonded original links, and no bonds on dual links which cross bonded original links. Now suppose that in the original lattice there was a site or cluster of sites that was not bonded to the main cluster. Then on the dual lattice, it would be surrounded by a closed loop of dual bonds. However it is easy to see that for this model it is impossible to construct such a closed loop. Since there is only one unbonded link per plaquette on the original lattice, there can only be one dual bond coming from any dual site at the center of a plaquette. It is therefore impossible to connect more than one dual bond, since that would require two dual bonds coming from the same dual site. Hence dual sites are only connected in pairs, by a single dual bond, and there is no possibility of making a closed loop of dual bonds.

Thus the SW algorithm bonds all the sites in the lattice together into a single cluster at the critical point, and so does not work for this model. However the generalized cluster algorithm of KBD, which deletes bonds using information on the state of plaquettes rather than links, works extremely well in this case [8, 10].

A. The KBD Algorithm

We will derive the KBD algorithm in a slightly different way, so as to make the generalization to other frustrated models more obvious, and to highlight the simple matrix methodology outlined in section II.

In the KBD algorithm, the tile used is a plaquette. There are seven freeze/delete operations, as shown in Fig. 1. Operations 2-7 conserve the energy of a configuration.

Note that operations 2-3 and operations 4-7 are just different orientations of the same basic topology of frozen and deleted bonds. To simplify matters, we will classify the operations into the 3 basic topologies (`A`, `B`, and `C` in Fig. 1) which we will refer to as *operators*. Each of the operators has some number of possible orientations: 1 for operator `A`, 2 for operator `B`, and 4 for operator `C`. However, the important feature of these operators for constructing a generalized cluster algorithm is the number of orientations that are possible for any given configuration of spins in a plaquette. For example, consider a plaquette having the lowest energy, $-2J$. This has one unsatisfied link. Since we can only freeze satisfied links, this means there is only one allowed orientation of operator `B` (the one with the deleted bonds corresponding to the unsatisfied link and the link parallel to it), and two allowed orientations of operator `C` (deleting the unsatisfied link and one of the links at right angles to it on either side).

Likewise, the important property of a plaquette configuration is not the spins, but rather which of the links are satisfied, since that alone determines which freeze/delete operations can be applied. From now on we will use the term "configuration" to mean a configuration of satisfied and unsatisfied links, rather than spins. Again, there are only a few basic topologies of satisfied and unsatisfied links – for the square lattice FFIM there are only two (either 1 or 3 unsatisfied links), in general there will be at least as many as there are possible energy states of the tile. All other configurations are just different orientations of these basic "link topologies".

To simplify matters, we will consider different orientations of the configurations and the freeze/delete operations to be equivalent. In order to use the matrix formalism outlined in section II, we need to know the number of different link topologies, and the number of allowed orientations n_{ij} of each operator i for any given configuration of link topology j. If we adopt this approach, the elements of the allowance matrix

A will be n_{ij}. The allowance matrix for the KBD algorithm is shown in Table I.

Solving equation 6 (which is easily done using Mathematica) gives the probabilities $P_i(j)$ given in Table II. Here the $P_i(j)$ refer to the probability of choosing operator i for a given configuration of link topology j. Each orientation of the operator which is allowed for the particular configuration would then be assigned with equal probability, $1/n_{ij}$. For example, if we chose operator `C`, we would randomly choose with probability $\frac{1}{2}$ to delete either of the 2 bonds perpendicular to the unsatisfied link.

Since for this model we have 3 operators and only 2 link topologies, the solution to the matrix equation has a free parameter p. KBD use this freedom in the choice of the probabilities to prove (using a subtle geometrical argument) that for a particular choice of probabilities, the lattice is always split into at least two large clusters at the zero temperature critical point [10]. For the probabilities chosen by KBD, the average maximum cluster size is neither too large nor too small (the average being 0.6432(5) for a 64^2 lattice), so the KBD cluster algorithm works extremely well.

When we set up the matrix equation, we could have treated all possible orientations of the configurations and the operators as different, rather than grouping them together as we have done. This would give 4 lowest energy configurations (rather than just 1), corresponding to the 4 possible positions of the single unsatisfied link in the plaquette. It would also give the 6 energy conserving operations of Fig. 1 (rather than the 2 basic operators). So instead of a single free parameter, from having 2 operators and only 1 configuration, there are now 2 free parameters, from having 6 operations and only 4 configurations. If we solve the extended matrix equation, we find that the free parameter enters (as one might expect) in the probability of choosing which of the bonds perpendicular to the unsatisfied link are to be deleted for operator `C`. We now have an extra probability p_{sub} of choosing the operations from the subgroup (4-5) of the angled operations, and $1 - p_{sub}$ of choosing the operations from the subgroup

(6-7), where previously we had $p_{sub} = \frac{1}{2}$.

Both these approaches – using the basic topologies or using all possible orientations – are correct, i.e. satisfy detailed balance. The first is simpler and allows an easier implementation of more complex problems where there are a large number of possible topologies and orientations; the other may provide some extra freedom in the choice of probabilities, that can allow some tuning to improve the performance of the algorithm, as we shall see in section III C.

Although the KBD algorithm satisfies detailed balance, it is not ergodic at zero temperature – that is, starting from a particular ground state configuration, it cannot generate all other ground state configurations. In fact, it can readily be seen for small lattice sizes that the KBD algorithm cycles between subsets of possible ground state configurations. In order for the algorithm to be ergodic, each KBD update must be followed by a Metropolis sweep. However, to our knowledge ergodicity of the Metropolis algorithm has not been *proven* for this model at zero temperature, although it is believed to be true (proving ergodicity is often a very difficult problem, see for example Ref. [15]). It can however be easily seen (again by just looking at test configurations on small lattices) that the Metropolis algorithm is *not* ergodic if the sites to be updated are chosen in serial (rather than random) order.

B. Dynamic Critical Exponents

KBD measured the dynamic critical exponent for the exponential autocorrelation time to be $z \approx 0.55$ for their algorithm [10], compared to $z \approx 2$ for the Metropolis algorithm (see Refs. [4, 5] for discussion and definitions of autocorrelation times and dynamic critical exponents). However they had very low statistics (100,000 sweeps) and fairly small lattice sizes (up to 128^2), and it has been seen for the Ising ferromagnet that it is very difficult to get an accurate determination of z from such data [16]. We have therefore obtained much better data for the autocorrelations for this algorithm, in order to get a better determination of the dynamic critical exponent.

We measured the normalized autocorrelation function

$$\rho_A(t) = \frac{< A(0)A(t) > - < A(0) >^2}{< A(0)A(0) > - < A(0) >^2} \tag{7}$$

for the magnetization ($A = M$) as well as the square and the absolute value of the magnetization ($A = M^2$ and $A = |M|$), and used this to extract exponential autocorrelation times τ_{exp}, via

$$\rho(t) \sim e^{-t/\tau_{exp}}, \tag{8}$$

as well as integrated autocorrelation times

$$\tau_{int} = \frac{1}{2} + \sum_{t=1}^{\infty} \rho_A(t), \tag{9}$$

that are relevant to the increase in the statistical error due to correlated configurations. Details of the methods we used for measuring the autocorrelations, doing the fits, and estimating the errors are given in Ref. [16].

In Table IV we give the results for the autocorrelation times of M^2 for different lattice sizes L up to $L = 256$. All the results are from at least 7.5×10^6 iterations (more for smaller lattice sizes). Fig. 2 shows a log-log plot of these results. Straight line χ^2 fits give $z_{int} = 0.28(1)$ and $z_{exp} = 0.66(5)$. The integrated autocorrelations also fit fairly well to a logarithm, so that z_{int} could also be zero. This uncertainty also occurs with the autocorrelations of cluster algorithms for the ferromagnetic Ising model [16], since it is very difficult to differentiate between a logarithm and a small power.

Let us define τ_0 to be the autocorrelation time obtained from an exponential fit to $\rho(t)$ at only two points, $t = 0$ and $t = 1$. This is also plotted in Fig. 2. We can see that τ_0 grows extremely slowly with L (slower than $\log(\log L)$ in fact), and seems to be approaching a constant value. This is in marked contrast to τ_{exp}, which grows as a substantial power of L. Unfortunately this makes it very difficult to get a good asymptotic fit to $\rho(t)$ at large t, since it has already fallen off so much at $t = 1$ that the signal is very small and noisy in the region where we need to fit to obtain τ_{exp}. The fact that τ_0 increases so slowly means that the τ_{int} grows much slower than τ_{exp}, and consequently z_{int} is much smaller than z_{exp}.

The reason that $\tau_{int} << \tau_{exp}$ is presumably that the operator M^2 does not have a large overlap with the slowest mode. The value of τ_{exp} should be independent of the operator measured, since it measures the relaxation of the slowest mode, however if there is not good overlap with this mode, this may mean that our estimate of τ_{exp} is not a good one. To get a better understanding of the dynamics of this system, one would need to find an operator for which $\tau_{int} \approx \tau_{exp}$. We also measured the autocorrelation times for the magnetization and the absolute value of the magnetization. For the former the results were zero for all lattice sizes, while the latter gave results almost identical to those given above for the square of the magnetization.

In almost every iteration of the standard KBD algorithm, the lattice is split into 2 clusters, and only rarely into 3 or more. The update consists of flipping the spins in a cluster with probability 1/2. If there are two clusters, this means that in half of the iterations either no spins are flipped, or all the spins are flipped, so there is no change in the configuration apart from a trivial global spin flip. Only half of the iterations make a non-trivial update of the configuration by updating one of the clusters and not the other. If there are 2 clusters, a more effective update scheme is to pick one of them at random and flip its spins. This guarantees that there are no "wasted" iterations. One would expect that this new update scheme would decrease the error in measurable quantities by a factor of $\sqrt{2}$, due to a decrease in τ_{int} by a factor of 2. However it turns out that the improvement is actually greater than this. The reason is that the the autocorrelation function for the new algorithm *alternates in sign*, as shown in Fig. 4. Thus using the definition for τ_{int} (equation 9) gives a value close to zero, and much less than half of the value for the standard KBD algorithm with an exponential autocorrelation function.

The autocorrelation function for a Markov process can generally be expressed asymptotically as $\rho(t) = a^t$, where $|a| < 1$ [17]. If $a > 0$, then redefining $a = e^{-1/\tau_{exp}}$ gives the standard asymptotic exponential form for $\rho(t)$. However it is also possible to have $a < 0$, in which case the autocorrelation function still falls off exponentially, but its sign is $(-1)^t$. This generally indicates that the original data forms an alternating time series, with successive measurements falling predominantly on one side and then the other of the mean value [17]. If $\rho(t) = a^t$, then $\tau_{int} = \frac{1}{2}\frac{1+a}{1-a}$, which can be very small for a negative. In order to calculate τ_{int} for the alternating autocorrelation function from the simulation data, we adopt a similar procedure to that used for the standard autocorrelation function [16]. We treat $\rho(2t)$ and $-\rho(2t+1)$ as separate positive functions, and fit them in the usual way to find τ^+_{exp} and τ^-_{exp}. These two values are very similar for this algorithm, as are the corresponding dynamic critical exponents $z^+_{exp} = 0.42(4)$ and $z^-_{exp} = 0.36(4)$, which are distinctly smaller than z_{exp} for the standard KBD algorithm. A logarithmic increase in τ_{exp} with lattice size (i.e. $z^{\pm}_{exp} = 0$) is also consistent with the data.

We can also calculate

$$\tau^+_{int} = \frac{1}{2} + \sum_{t=1}^{\infty} \rho(2t),$$
$$\tau^-_{int} = -\sum_{t=0}^{\infty} \rho(2t+1), \qquad (10)$$

in the usual way by by splitting each infinite sum into a small t finite sum plus the remaining large t infinite sum, which can be summed analytically using the fact that the autocorrelation functions fall off asymptotically as $Ae^{-t/\tau_{exp}}$. This gives

$$\tau^+_{int} = \frac{1}{2} + \sum_{t=1}^{W^+} \rho(2t) + \frac{A^+ e^{-2(W^+ +1)/\tau^+_{exp}}}{1 - e^{-2/\tau^+_{exp}}},$$
$$\tau^-_{int} = \sum_{t=0}^{W^-} \rho(2t+1) + \frac{A^- e^{-[2(W^- +1)+1]/\tau^-_{exp}}}{1 - e^{-2/\tau^-_{exp}}}, \tag{11}$$

where the windows W^+ and W^- are taken to be the end of the region where we fit for τ_{exp}. Now we can obtain the integrated autocorrelation time for the alternating $\rho(t)$ as

$$\tau_{int} = \tau^+_{int} - \tau^-_{int}. \tag{12}$$

The integrated autocorrelation times for this method are shown in Fig. 2. They are smaller than for the standard KBD algorithm, however the dynamic critical exponent $z_{int} = 0.32(2)$ is approximately the same, and could also be zero.

Another interesting result concerns the autocorrelation function $\rho(t)$ for the KBD algorithm *without* the Metropolis sweep needed for ergodicity, which is shown in Fig. 5, along with $\rho(t)$ for the algorithm *including* Metropolis sweeps. The latter falls off asymptotically as an exponential, as expected, while $\rho(t)$ for the non-ergodic algorithm asymptotes to a logarithm. This implies that the autocorrelation time is infinite, which one might expect for a non-ergodic algorithm (although it is not clear why $\rho(t)$ should have a perfectly logarithmic form). However, measuring the autocorrelation function at zero temperature cannot tell us whether an algorithm is ergodic. For example, the Metropolis algorithm implemented so that the sites are visited in serial order is also a non-ergodic algorithm for this model, although we found that its autocorrelation function was asymptotically exponential, and in fact has a much *smaller* apparent autocorrelation time than the algorithm with the sites chosen in random order, which is presumed to be ergodic. In this case the non-ergodic algorithm has smaller correlations between successive configurations, but only generates a subset of all possible configurations.

C. A Variant of the KBD Algorithm

In order to guarantee that the lattice is broken up into at least 2 large clusters at zero temperature, KBD used the freedom in choosing the probabilities so that only operations 2 and 3 of Fig. 1 had non-zero probability at $T = 0$. However in order to investigate the effect of tuning the extra free parameter p_{sub}, we used an alternate version of the KBD algorithm that uses only the angle operations (4-7) at zero temperature, rather than the operations (2,3) used by KBD. We measured the cluster sizes and autocorrelations for this algorithm for different values of p_{sub}: 1.0, 0.8, and 0.5. As noted by KBD, for this choice of probabilities the lattice is no longer split into two large clusters, rather we get one very large cluster and a number of very small clusters. Tuning this extra free parameter does have an effect on the largest cluster size, although it is quite small: the average maximum cluster size is 0.91762(1) of the lattice for $p_{sub} = 0.5$, 0.89978(6) for $p_{sub} = 0.8$, and 0.87371(10) for $p_{sub} = 1.0$. For $p_{sub} = 1.0$ the geometry of the operators is such that all sites are either in a single site cluster or part of a spanning cluster (the largest cluster).

Integrated autocorrelation times for these three variations of the KBD algorithm are shown in Fig. 3, along with results for the Metropolis algorithm, and the KBD results from Fig 2. The results are quite surprising. As expected, $p_{sub} = 0.5$ gives a value $z = 1.97(2)$ which is very similar to the Metropolis algorithm, since the largest cluster encompasses most of the lattice and consequently the cluster update does little apart from a global spin flip. For larger values of p_{sub} we have seen that the biggest cluster size is reduced very slightly, however this is enough to substantially reduce the autocorrelations: $p_{sub} = 0.8$ has $z = 0.62(2)$, while $p_{sub} = 1.0$ has $z = 0.48(1)$. It is very surprising that in going from $p_{sub} = 0.5$ to 1.0 the biggest cluster size is only reduced by about 5%, yet z is reduced from around 2.0 to around 0.5! This result is very promising, since it implies that critical slowing down can be substantially reduced even when the biggest cluster size is quite large (87% of the lattice in this case), so for other frustrated spin models we may not have to unfreeze the lattice very much to get good results.

Our result is also surprising in that z appears to vary continuously between the Metropolis and KBD values. Based on the ideas of dynamic universality, it is more likely that there is a critical value of p_{sub} for which z jumps from one value (Metropolis) to the other (KBD). We have used rather small lattices ($L \leq 64$) for our analysis, so it is quite possible that the true value of z is actually the same for $p_{sub} = 0.8$ and $p_{sub} = 1.0$.

The generalized cluster algorithm works extremely well for the square lattice FFI, almost completely eliminating critical slowing down. However it is not clear that it can be successfully applied to other frustrated models. It is only by a fortuitous geometrical happenstance that the standard KBD algorithm is able to split the lattice into two large clusters at the critical point, and the algorithm we have investigated which uses only the angled operations works well only because it has a tunable parameter p_{sub} that allows the maximum cluster size to be reduced just enough to give a greatly reduced z. We were therefore interested to see whether the generalized cluster algorithms would work for other frustrated spin models.

IV. THE TRIANGULAR LATTICE ISING ANTIFERROMAGNET

We first attempted to apply the KBD cluster algorithm to an even simpler fully frustrated model, the anti-ferromagnetic Ising model on a triangular lattice. This model is very similar to the square lattice FFIM, being in the same universality class and also having a critical point at zero temperature [18, 19].

The ground state of this model has only one unsatisfied link per triangular plaquette. The SW algorithm puts a bond on all satisfied links, so we can apply the same argument as for the square lattice FFIM to see that the SW algorithm again freezes the lattice into a single cluster at zero temperature.

We can get some idea of the percentage of bonds that need to be deleted to break up this single cluster by noting that the bond percolation threshold for a triangular lattice is 0.35792 [20]. For the square lattice the bond percolation threshold is 0.5 [20], which is also the ratio of frozen bonds to links in the KBD algorithm for the square lattice FFIM at the zero temperature critical point. This is of course only a rough pointer to what is required, since for bond percolation the bonds are placed on the lattice at random, whereas for the KBD algorithm on the square lattice we must have two bonds for each plaquette at zero temperature. Even with the bond/link ratio being the same as the percolation threshold, the largest cluster for the KBD algorithm percolates at a temperature well above the critical point.

A. The Plaquette Algorithm

The application of the KBD algorithm to the triangular lattice FFIM is very simple. As with the square lattice, we choose the basic element to be a (triangular) plaquette, which has two possible energy states, $+J$ and $-J$. For the triangular lattice there are only four possible freeze/delete operations, which are shown in Fig. 6. We can either delete all the bonds, or delete one of the two satisfied bonds. Since the ground state configuration has a single unsatisfied link, and the energy conserving operations (2-4 of Fig. 6) freeze a single bond, there are 3 possible orientations of each. Thus, unlike the square lattice case, there are no free parameters when we solve the matrix equation 6, even when all possible orientations of the configurations and operations are used. The probabilities for each operation are given in Table V.

At the zero temperature critical point, we only perform the energy conserving operations (2-4). This gives a bond/link ratio of $\frac{1}{3}$, which is below the percolation threshold for the triangular lattice, although in this case the bonds are not placed randomly, but rather one per plaquette. However we expect to at least be able to create multiple clusters, as with the KBD algorithm with angled operations for the square lattice FFIM.

We tested this algorithm at zero temperature, following every cluster update by a Metropolis sweep to ensure ergodicity. We found that the algorithm produces one very large cluster, and a number of very small clusters. For a 64^2 lattice there are an average of 205.1(1) clusters, with the average size of the largest cluster being 0.9233(1) of the lattice volume. This is very similar to the results for the square lattice case using the angled operations with equal probability. In that case there is a free parameter (p_{sub}) that allows us to bias the choice of the operations so as to reduce the largest cluster size and greatly improve the performance of the algorithm. However for the triangular lattice there is no such freedom, and in order to satisfy detailed balance the two possible energy conserving operations for each plaquette must be chosen with equal probability. We checked that introducing a bias in the choice of the operations (2-4) does indeed reduce the largest cluster size, but of course it also gives incorrect results due to the violation of detailed balance.

Since the ground state for this model is paramagnetic, we measured the paramagnetic susceptibility $\chi = V < M^2 >$, where M is the average magnetization per site, and V is the lattice volume. At the zero temperature critical point, this quantity approaches a constant value as the lattice size is increased. We also measured the spin correlation function $\Gamma(R) =< \sigma_0 \sigma_R >$ (which is known exactly for an infinite lattice [21]) at a distance $R=2$. We measured the autocorrelations in χ and $\Gamma(2)$ for both the plaquette algorithm and the standard Metropolis algorithm. The autocorrelation times for the plaquette algorithm were doubled to give a fairer comparison with the Metropolis algorithm, since every iteration of the plaquette algorithm includes a

Metropolis update to ensure ergodicity.

The integrated and exponential autocorrelation times for the Metropolis and plaquette algorithms for χ are shown in Fig. 7, and for $\Gamma(2)$ in Fig. 8. Even for the Metropolis algorithm, the autocorrelations are quite small, and grow much slower than L^2. The plaquette algorithm seems to almost completely eliminate critical slowing down in the measurement of χ, although this is not much of an improvement over Metropolis. However the plaquette algorithm substantially reduces the autocorrelations for $\Gamma(2)$, especially τ_{exp}, which is related to the time required to thermalize to a ground state configuration. Notice that τ_{exp} is different for the different operators. Again, this means that M^2 (and possibly also $\Gamma(2)$) does not have a large overlap with the slowest mode, so our measurements of this quantity are presumably quite poor. Again, one would like to find an operator for which $\tau_{int} \approx \tau_{exp}$. The dynamic critical exponents for χ and $\Gamma(2)$ for the two Monte Carlo algorithms are shown in Table VI.

It is possible to construct a simple plaquette generalized cluster algorithm for the triangular lattice FFIM that is certainly superior to the standard Swendsen-Wang cluster algorithm, which freezes the lattice into a single cluster and is therefore totally ineffective. The size of the biggest cluster in the plaquette algorithm is still very large, and there are no tunable parameters that might enable us to reduce it, although it appears that the algorithm performs well in spite of this problem. However this may just be an fortuitous anomaly, since even the Metropolis algorithm performs quite well for the quantities which we measured. We therefore tried to find a general method for improving the generalized cluster algorithm by further decreasing the size of the largest cluster.

B. A Larger Tile Algorithm

To try to improve on this algorithm, we investigated making the tile something larger than a plaquette. Since increasing the tile from a single link (Swendsen-Wang) to a plaquette (KBD) improves the low temperature algorithm substantially, it is possible that an even larger tile will produce better results. Note that the simple double plaquette shown in Fig. 9(a) cannot tile the lattice – that is, it is not possible to cover all the links in the lattice such that each link is uniquely assigned to a double triangular plaquette. Since the double plaquette has only 5 links and the number of links in the lattice is a multiple of 3, there is an extra link required. Fig. 9(b) shows a set of links that can tile a triangular lattice.

For this model a ground state configuration has two satisfied links in each triangular plaquette. There are 8 configurations of the tile that can occur in the ground state, which are shown in Fig. 10. Unlike the algorithm using the triangular plaquette, these ground state configurations of the tile can have different energies.

An operation conserves energy if it freezes at least one satisfied bond for each triangular plaquette. For this tile, there are 17 possible energy conserving operations that freeze 3 or fewer bonds. These are shown in Fig. 11, along with the single allowed operation that freezes 5 bonds, and one of the 5 possible operations that freeze four bonds. Note that operations 14-18 (and the other 4-bond operations that are not shown) are equivalent in the sense that they ensure the same 4 sites are bonded together into the same cluster, so there is no reason to choose one in preference to another. Note that there is a subtlety here in what we mean by an energy conserving operation. These operations ensure that the total energy of a ground state configuration is unchanged, as it should be at zero temperature. However the energy of a *tile* can take three different values for a given ground state configuration: $-4J$, $-2J$ and 0. The energy conserving operations may change the energy of a tile, but they will not change the total energy of the configuration (summed over all tiles).

It is quite straightforward to choose a subset of the possible operations in Fig. 11 which give an upper triangular allowance matrix, as shown in Table VII. Since we have many more operations than configurations, it is possible to choose some redundant operations which add free parameters to the probabilities. For simplicity we have only chosen one (operation 6), however there are other possible choices which would add extra parameters. Solving the matrix equation gives the probabilities in Table VIII, which give a valid algorithm at zero temperature. Notice that if we choose to set the free parameter $p_2 = 1$, the algorithm is greatly simplified and only involves a few operations (1, 2, 4, 18, 19), since the probabilities for the other operations are zero. The first three of these freeze only 2 bonds per tile, thus giving the same bond/link ratio as the single plaquette algorithm. The problem with this algorithm is that in order to get an upper triangular allowance matrix (and thus sensible probabilities), we need to choose 2 operations (18 and 19) which freeze *all* the bonds in configurations 7 and 8, which make up a substantial proportion of the tiles at zero temperature. This means that the algorithm with this larger tile has a greater bond/link ratio than the single plaquette algorithm. Any choice of the other operations and free parameters will suffer the same problem.

One subtlety in this algorithm is the choice of tiling at each iteration. For the single plaquette algorithm there are two possible tilings of the triangular lattice, just as there are for the square lattice algorithm, and one of the two possibilities (either the black or white squares in a checkerboard pattern) are chosen at random for each iteration. However in this case the tile of Fig. 9(b) is asymmetric, so the number of different tilings is 12, since there are 6 possible ways the link coming off the double plaquette can be oriented, and 2 possible ways of partitioning the lattice (the black and white partitioning) for each of these orientations. One of the 12 possible tilings is chosen at random for each iteration.

We found that the larger bond/link ratio of this algorithm produced a single cluster covering the whole lattice at zero temperature. We tried some variations, such as taking $p_2 < 1$, and trying different operations, but got the same result. Thus the generalized cluster algorithm with a larger tile does even worse than the single plaquette algorithm for the FFIM on a triangular lattice.

V. OTHER 2-D FRUSTRATED MODELS

Let us consider the $\pm J$ Ising spin glass, where the couplings J_{ij} in equation 1 are chosen to be ferromagnetic ($+J$) or antiferromagnetic ($-J$) at random [7]. For the spin glass the generalization of the KBD algorithm at the zero temperature critical point is very simple. For plaquettes with an even number of ferromagnetic links, we must freeze all the satisfied links in order to conserve energy, so this is the same as the SW algorithm. For plaquettes with an odd number of ferromagnetic links, we have the KBD algorithm for the FFIM.

For the spin glass there is not the regular geometry that allows the KBD algorithm to split the lattice into two clusters for the FFIM, and at zero temperature this combined KBD/SW algorithm freezes the lattice into a single cluster. It is possible that a workable generalized cluster algorithm may be constructed for this model using a larger tile than the plaquette, however as we have seen this was not the case for the triangular lattice FFIM.

VI. CONCLUSIONS

One of the main ideas of KBD was to extend the basic element of a cluster algorithm from a link connecting only two sites to a larger geometrical object such as a plaquette. This is clearly necessary for frustrated systems, for which knowledge of the frustration of the system cannot be obtained from looking at the interaction of two neighboring spins. We have presented a simplified method for constructing a generalized cluster algorithm for an arbitrary spin model based on any group of spins that can tile the lattice.

However for a particular spin model, there is no guarantee that a valid algorithm with sensible probabilities for each possible freeze/delete operation can be constructed. Even if such an algorithm does exist, the resulting clusters may still be too large, causing poor performance. For the 2-d Ising spin glass we found that a generalized cluster algorithm froze the lattice into a single cluster at zero temperature. For the triangular lattice FFIM the method produced a very large cluster, however the algorithm still appeared to work well. We have also used this method to construct a generalized cluster algorithm for the 3-d cubic lattice FFIM, which also produces a very large cluster at the critical point, and performs no better than the Metropolis algorithm [22].

Even when the plaquette algorithms do not perform well, they are still a great improvement over the Swendsen-Wang algorithm, which is the single-link version of the generalized cluster algorithm. It is possible that using tiles even larger than a plaquette will improve matters further, however we found that for the case of the triangular lattice FFIM this produced an algorithm which froze the lattice into a single cluster at zero temperature, and was therefore worse than the smaller tile algorithm.

The method we have used here is a more convenient, but specialized, case of the KBD generalized cluster algorithm. In particular, we have looked only at the case where the bonds are either frozen or deleted. This produces clusters that can be updated independently of one another. However the generalized cluster algorithm allows for another possibility, in which there is an interaction energy between the clusters.

This could allow the creation of smaller clusters that may be updated with a probability dependent on the energies of the other clusters, in a fashion similar to the algorithms of Niedermayer [23] and D'Onorio de Meo *et al.* [24]. However these kinds of interacting cluster algorithms have not proven to be effective for non-frustrated systems, mainly because the probability of updating a cluster is approximately inversely proportional to the exponential of the cluster size. Thus updating large clusters occurs with a very small probability, so these algorithms tend to be not much better than standard local Monte Carlo methods, at a much greater computational cost.

Although the generalized cluster algorithm seems very promising as an approach to simulating frustrated systems, and works very well for simple two dimensional fully frustrated Ising models, it does not appear to be generally applicable to any spin model. Just constructing clusters to update so as to satisfy detailed balance does not appear to be enough – cluster algorithms only seem to work when the clusters are constructed in a way which reflects the physics of the model. Thus different algorithms are required for different models, and finding a general algorithm which works in all cases seems a daunting task. We have not tried all possible choices of operations and parameters for this method, however from our experience it appears that just tuning parameters will not work, and some new ideas are necessary before generalized cluster algorithms can be successfully applied to more complicated frustrated systems such as spin glasses and models in more than two dimensions.

ACKNOWLEDGMENTS

We are grateful to John Apostolakis, Ofer Biham, Danny Kandel, Enzo Marinari and Alan Sokal for valuable discussions. This work was sponsored in part by Department of Energy grants DE-FG03-85ER25009 and DE-AC03-81ER40050, and by a grant from the IBM corporation.

NOTE ADDED

After this work was completed, we obtained the University of Marburg preprint "Cluster mechanisms in the fully frustrated Ising model", by Werner Kerler and Peter Rehberg (cond-mat/9401063), which addresses many similar issues to the work described here.

REFERENCES

[1] R.H. Swendsen and J.-S. Wang, Phys. Rev. Lett. **58**, 86 (1987); J.-S. Wang and R.H. Swendsen, Physica A **167**, 565 (1990).

[2] U. Wolff, Phys. Rev. Lett. **62**, 361 (1989).

[3] N. Metropolis *et al.*, J. Chem. Phys. **21**, 1087 (1953).

[4] K. Binder ed., *Monte Carlo Methods in Statistical Physics*, (Springer-Verlag, Berlin, 1986); K. Binder and D.W. Heermann, *Monte Carlo Simulation in Statistical Physics*, (Springer-Verlag, Berlin, 1988); H. Gould and J. Tobochnik, *An Introduction to Computer Simulation Methods, Vol. 2*, (Addison-Wesley, Reading, Mass., 1988).

[5] A.D. Sokal, in *Computer Simulation Studies in Condensed Matter Physics: Recent Developments*, eds. D.P. Landau *et al.* (Springer-Verlag, Berlin-Heidelberg, 1988); A.D. Sokal, in Proc. of the International Conference on Lattice Field Theory, Tallahassee, October 1990, Nucl. Phys. B (Proc. Suppl.) **20**, 55 (1991).

[6] G. Toulouse, Commun. Phys. **2**, 115 (1977).

[7] K. Binder and A.P. Young, Rev. Mod. Phys. **58**, 801 (1986); D. Chowdhury, *Spin Glasses and Other Frustrated Systems*, (Princeton University Press, Princeton, NJ, 1986); M. Mezard and G. Parisi, *Spin Glass Theory and Beyond*, (World Scientific, Singapore, 1987).

[8] D. Kandel, R. Ben-Av and E. Domany, Phys. Rev. Lett. **65**, 941 (1990).

[9] D. Kandel and E. Domany, Phys. Rev. B **43**, 8539 (1991).

[10] D. Kandel, R. Ben-Av and E. Domany, Phys. Rev. B **45**, 4700 (1992).

[11] R.H. Swendsen and J.-S. Wang, Phys. Rev. Lett. **57**, 2607 (1986).

[12] R.H. Swendsen and J.-S. Wang, Phys. Rev. B **38**, 4840 (1988).

[13] S. Wolfram, *Mathematica: a system for doing mathematics by computer*, (Addison-Wesley, Redwood City, Calif., 1990).

[14] J. Villain, J. Phys. C **10**, 1717 (1977).

[15] M. Lubin and A.D. Sokal, Phys. Rev. Lett. **71**, 1778 (1993).

[16] C.F. Baillie and P.D. Coddington, Phys. Rev. B **43**, 10617 (1991).

[17] M.B. Priestley, *Spectral Analysis and Time Series*, (Academic Press, London, 1981).

[18] G.H. Wannier, Phys. Rev. **79**, 357 (1950).

[19] J. Stephenson, J. Math. Phys. **11**, 420 (1970).

[20] D. Stauffer, *Introduction to Percolation Theory*, (Taylor and Francis, London, 1985).

[21] J. Stephenson, J. Math. Phys **5**, 1009 (1964).

[22] P.D. Coddington and L. Han, "A generalized cluster algorithm for the 3-d fully frustrated Ising model", NPAC technical report SCCS-528.

[23] F. Niedermayer, Phys. Rev. Lett. **61**, 2026 (1988).

[24] M. D'Onorio de Meo, D.W. Heermann and K. Binder, J. Stat. Phys. **60**, 585 (1990).

TABLES

TABLE I. Matrix containing the number of possible orientations of the freeze/delete operators of Fig. 1 for each energy state of the the square lattice FFIM.

		Operators		
Energy	Config	`A`	`B`	`C`
$-2J$	1	1	1	2
$2J$	2	1	0	0

TABLE II. Probabilities for the freeze/delete operators of Fig. 1 for the square lattice FFIM.

		Operators		
Energy	Config	`A`	`B`	`C`
$-2J$	1	e^{-4K}	p	$1 - e^{-4K} - p$
$2J$	2	1	0	0

TABLE III. The average size of the maximum cluster (as a ratio of the lattice volume) and the other clusters (given as a number of sites), and the average number of clusters, for different values of the free parameter p_{sub} for the KBD algorithm using the angled operations (4-7) for the square lattice FFIM at zero temperature on a 64^2 lattice. Also shown are the values for the standard KBD algorithm using only operations (1-3).

p_{sub}	0.5	0.8	1.0	KBD
Size of Largest Cluster	0.91760(2)	0.89970(1)	0.87362(2)	0.6432(5)
Size of Other Clusters	1.204	1.11	1.00	708
Number of Clusters	280.22(6)	370.18(4)	518.64(6)	2.0603(7)

TABLE IV. Autocorrelation times of M^2 for the standard KBD algorithm applied to the square lattice FFIM at zero temperature.

L	$\tau_{int}(M^2)$	$\tau_{exp}(M^2)$
8	0.888(1)	0.977(9)
16	1.035(2)	1.85(3)
32	1.265(2)	3.60(6)
64	1.539(4)	5.9(1)
128	1.849(7)	9.3(2)
256	2.188(16)	13.7(5)

TABLE V. Probabilities for the freeze/delete operations of Fig. 6 for the triangular lattice FFIM.

		Operations	
Energy	Config	1	2
$-J$	1	e^{-4K}	$1-e^{-4K}$
$3J$	2	1	0

TABLE VI. Dynamic critical exponents for the Metropolis and plaquette algorithms for applied to the triangular lattice FFIM at zero temperature.

	Metropolis	Plaquette
$z_{int}(\chi)$	0.12(5)	0.04(3)
$z_{exp}(\chi)$	0.24(8)	0.08(5)
$z_{int}(\Gamma(2))$	0.52(5)	0.12(3)
$z_{exp}(\Gamma(2))$	0.70(10)	0.39(10)

TABLE VII. The allowance matrix for the freeze/delete operations of Fig. 11 for the triangular lattice FFIM at zero temperature.

		Operations								
Energy	Config	1	4	2	6	8	5	10	18	19
$-4J$	1	1	1	0	0	0	1	0	1	1
$-2J$	2	1	1	0	0	0	0	0	1	0
$-2J$	3	0	1	1	1	0	0	1	0	0
$-2J$	4	1	0	1	0	1	1	0	0	0
$-2J$	5	0	0	1	0	1	0	0	0	0
$-2J$	6	0	0	1	1	0	0	0	0	0
0	7	0	1	0	0	0	0	0	0	0
0	8	1	0	0	0	0	0	0	0	0

TABLE VIII. Probabilities for the freeze/delete operations of Fig. 11 for the triangular lattice FFIM at zero temperature.

		Operations								
Energy	Config	1	4	2	6	8	5	10	18	19
$-4J$	1	0	0	0	0	0	0	0	0	1
$-2J$	2	0	0	0	0	0	0	0	1	0
$-2J$	3	0	0	p_2	$1-p_2$	0	0	0	0	0
$-2J$	4	0	0	p_2	0	$1-p_2$	0	0	0	0
$-2J$	5	0	0	p_2	0	$1-p_2$	0	0	0	0
$-2J$	6	0	0	p_2	$1-p_2$	0	0	0	0	0
0	7	0	1	0	0	0	0	0	0	0
0	8	1	0	0	0	0	0	0	0	0

FIGURES

FIG. 1. Freeze/delete operations for the square lattice FFIM. The bold lines indicate frozen bonds.

FIG. 2. Log-log plot of the autocorrelation times of M^2 for the standard KBD algorithm for the square lattice FFIM at zero temperature.

FIG. 3. Log-log plot of τ_{int} of M^2 for the square lattice FFIM at zero temperature, using the Metropolis algorithm, the standard KBD algorithm, the new improved KBD algorithm where a cluster is flipped at every iteration, and the KBD algorithm using just angled operations with three different values of the free parameter p_{sub}.

FIG. 4. Autocorrelation function for the improved KBD algorithm for the FFIM on a 64^2 lattice at zero temperature.

FIG. 5. Autocorrelation functions of M^2 for the square lattice FFIM at zero temperature on a 64^2 lattice for the KBD algorithm with and without Metropolis sweeps, with asymptotic fits to an exponential and a logarithm respectively.

FIG. 6. Freeze/delete operations for the triangular lattice FFIM. The bold lines indicate frozen bonds.

FIG. 7. Autocorrelation times for χ at $T=0$ for the triangular lattice FFIM using the Metropolis and plaquette algorithms.

FIG. 8. Autocorrelation times for $\Gamma(2)$ at $T=0$ for the triangular lattice FFIM using the Metropolis and plaquette algorithms.

FIG. 9. Extensions of basic triangular plaquette: (a) double plaquette, (b) double plaquette plus extra link.

FIG. 10. Possible ground state configurations of the tile shown in Fig. 9(b). Here solid lines denote satisfied bonds.

FIG. 11. Possible energy conserving operations for the tile shown in Fig. 9(b). The bold lines indicate frozen bonds.

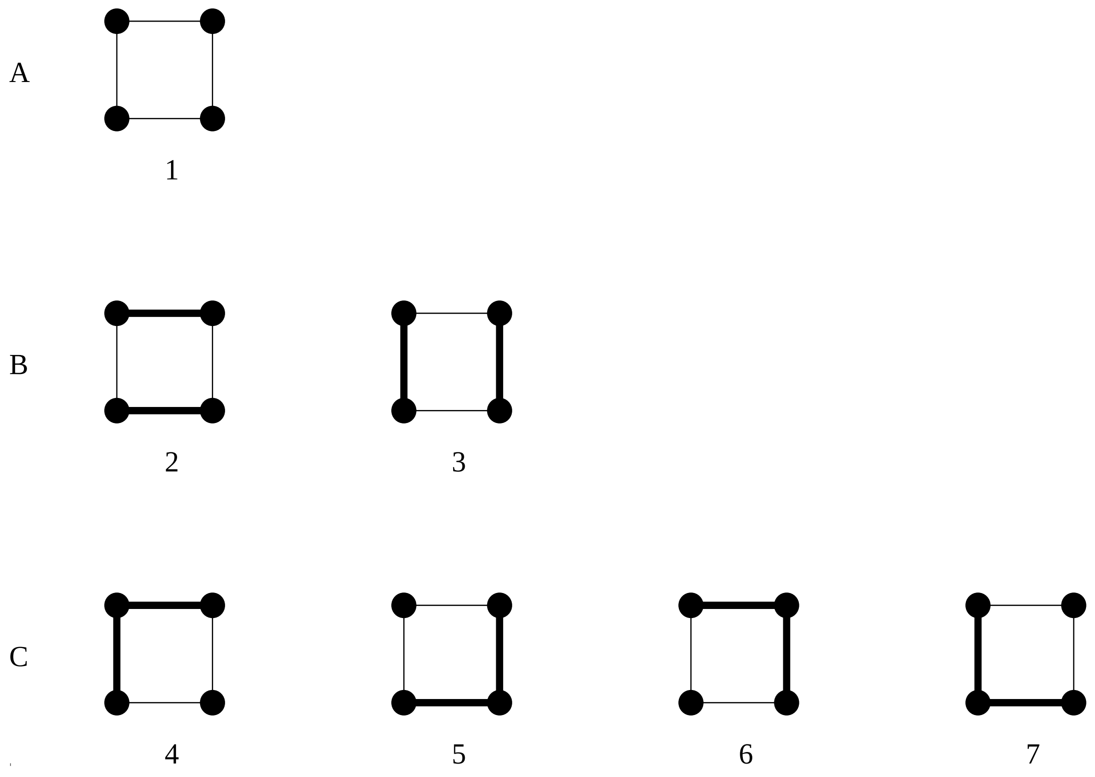

Fig. 1.

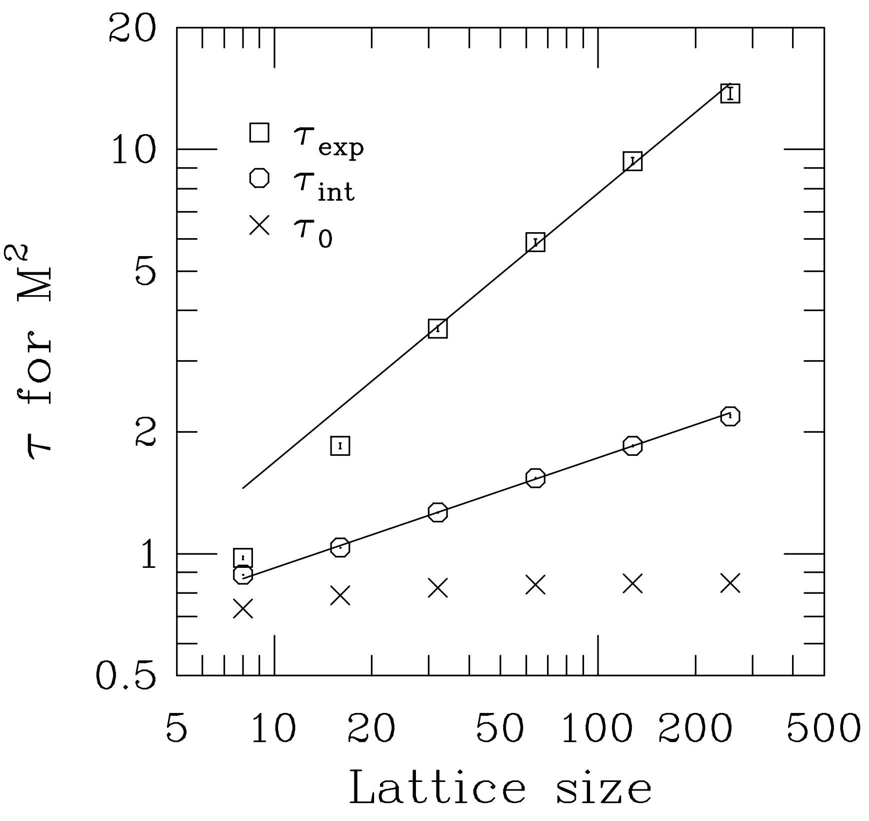

$\tau_{\rm exp}$
$\tau_{\rm int}$
τ_0
τ for M^2
Lattice size
20
10
5
2
1
0.5
5
10
20
50
100
200
500

Fig. 2.

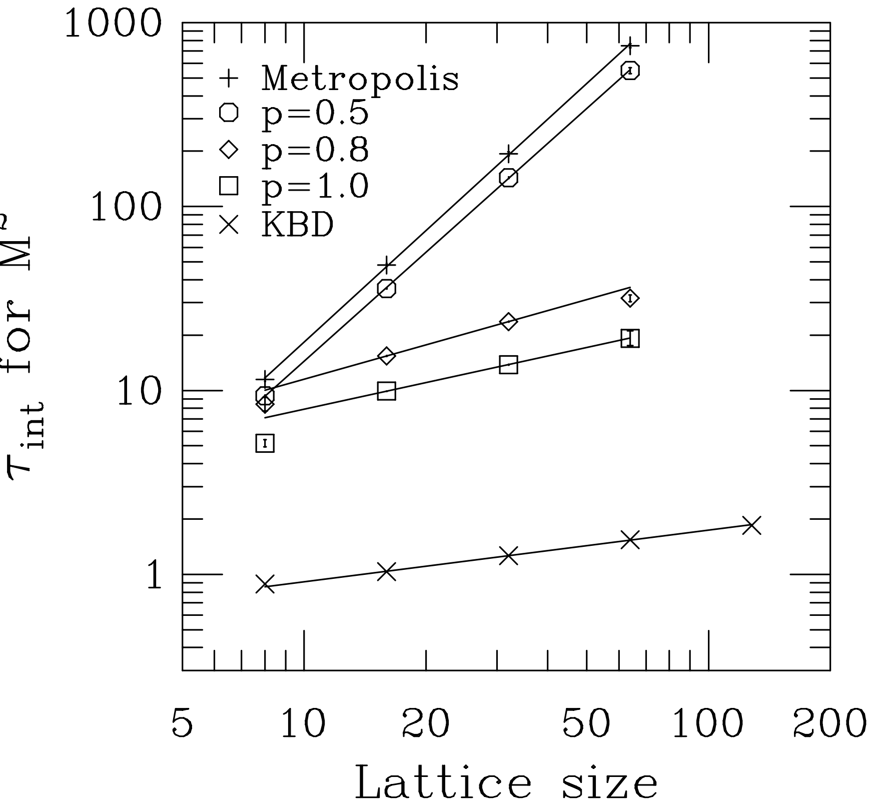

1000
100
10
1
5
10
20
50
100
200
+ Metropolis
○ p=0.5
◇ p=0.8
□ p=1.0
× KBD
τ_{int} for M^2
Lattice size

Fig. 3.

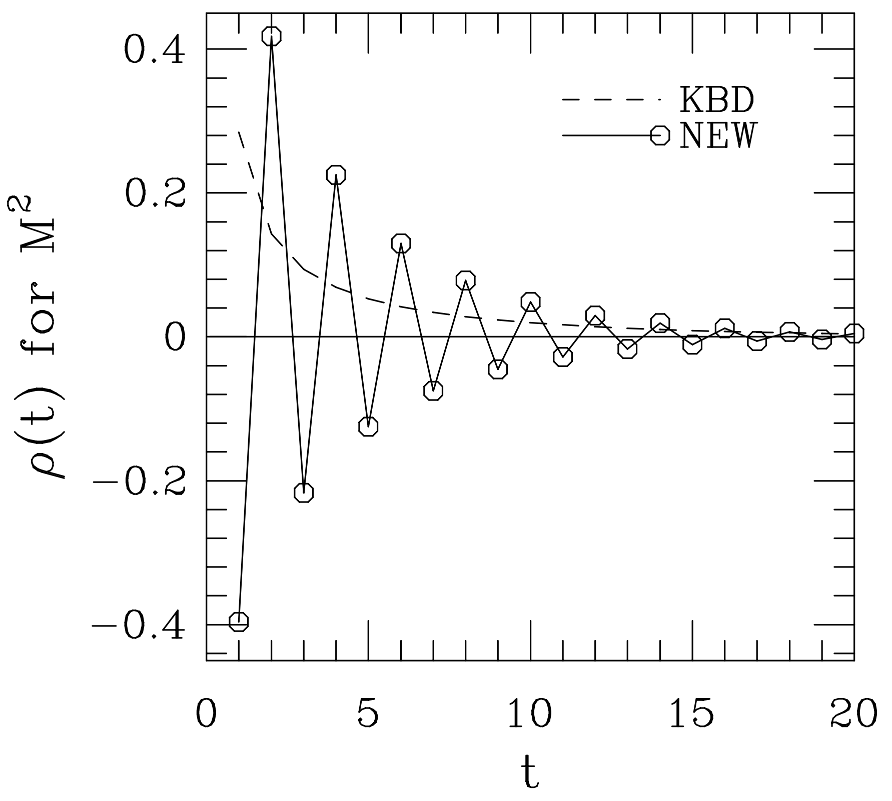

Fig. 4.

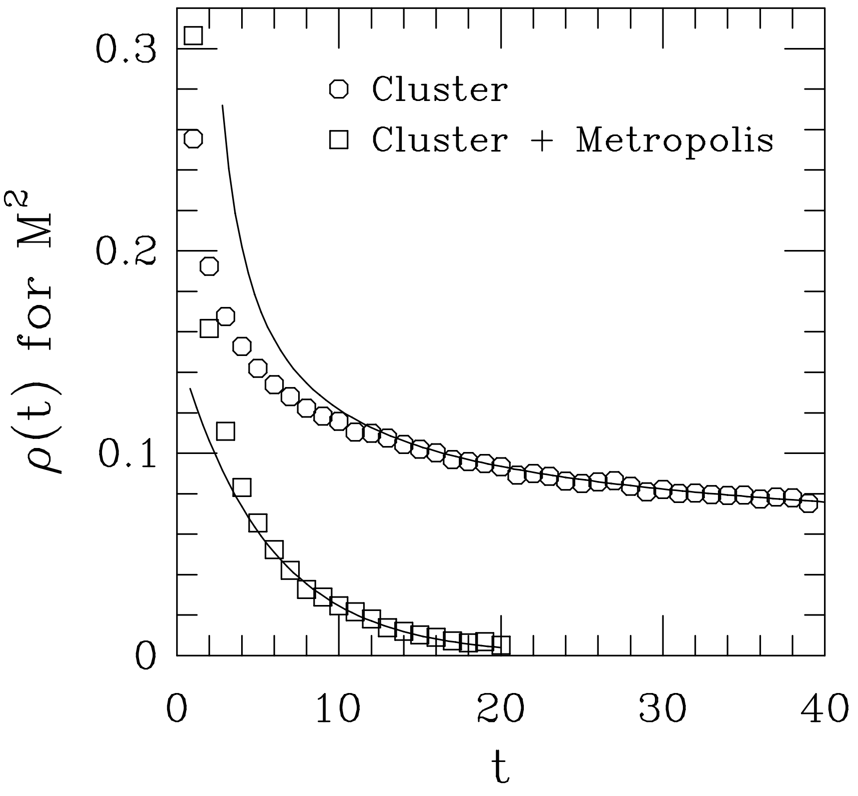

ρ(t) for M²
t
Cluster
Cluster + Metropolis
0
0.1
0.2
0.3
0
10
20
30
40

Fig. 5.

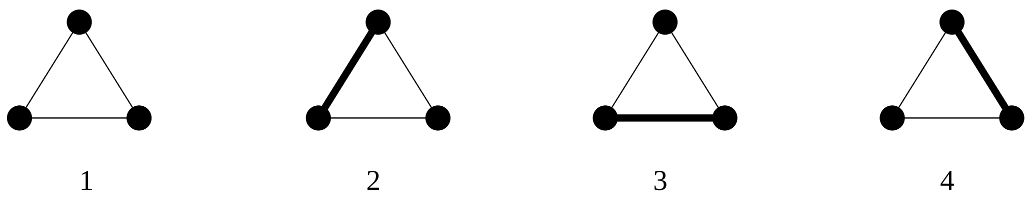

1
2
3
4

Fig. 6.

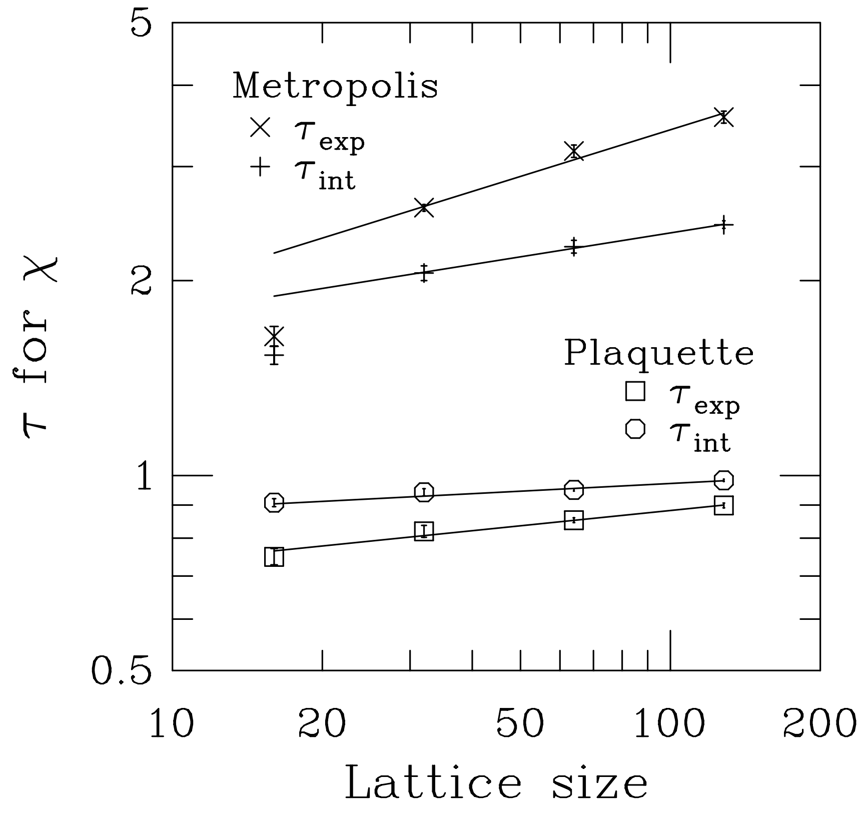

Metropolis
τ_{exp}
τ_{int}
Plaquette
τ_{exp}
τ_{int}
τ for χ
Lattice size
5
2
1
0.5
10
20
50
100
200

Fig. 7.

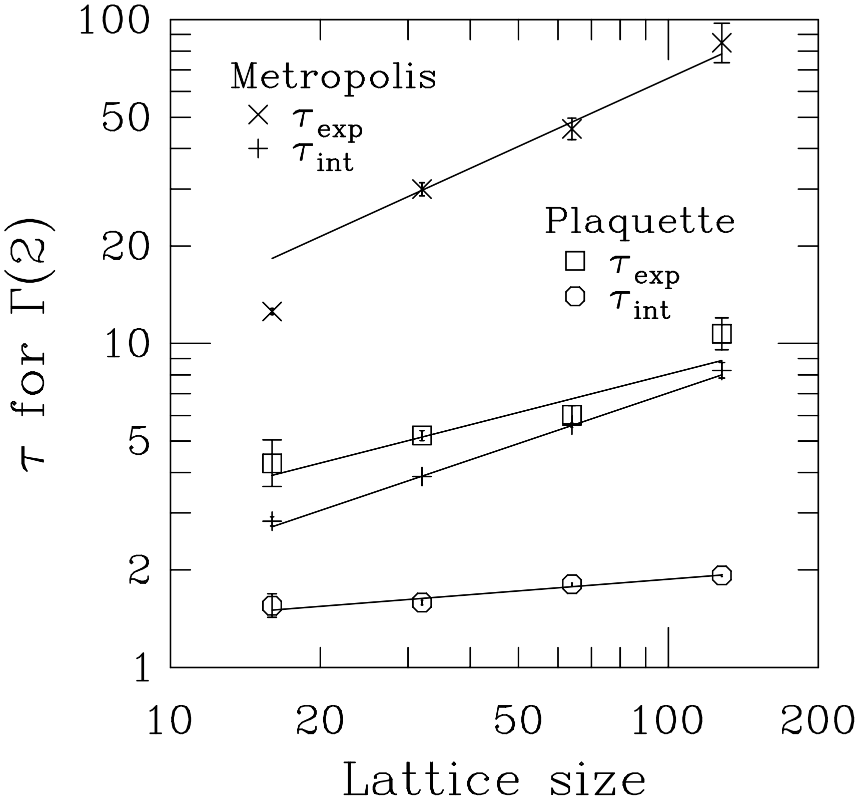

Metropolis
$\times$ $\tau_{\rm exp}$
$+$ $\tau_{\rm int}$
Plaquette
□ $\tau_{\rm exp}$
○ $\tau_{\rm int}$
τ for $\Gamma(2)$
Lattice size
100
50
20
10
5
2
1
10
20
50
100
200

Fig. 8.

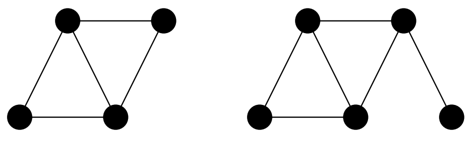

(a)
(b)

Fig. 9.

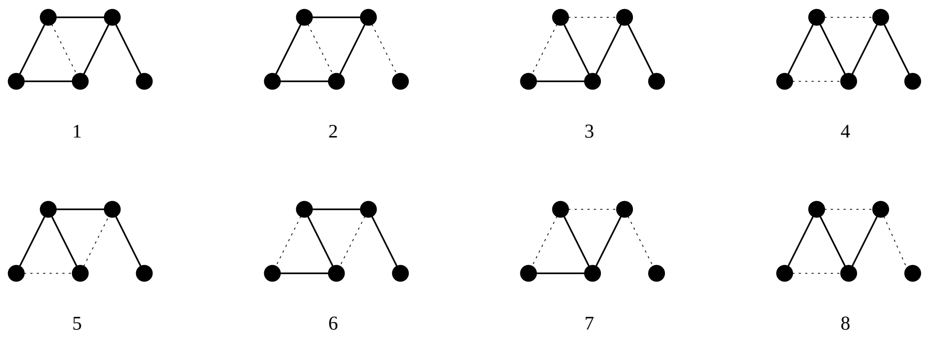

Fig. 10.

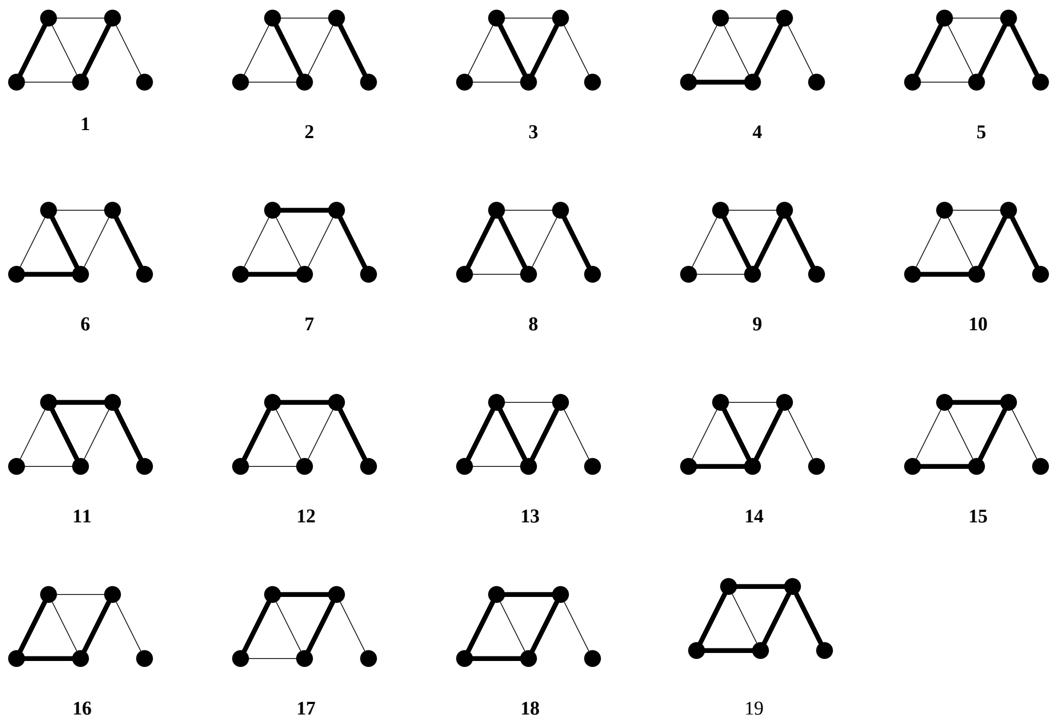

Fig. 11.